V.D.8 Molecular-Scale, Three-Dimensional Non-Platinum Group Metal Electrodes for Catalysis of Fuel Cell Reactions

John B. Kerr[1] (Primary Contact), Piotr Zelenay[2], Steve Hamrock[3]

[1]Lawrence Berkeley National Laboratory (LBNL)
MS 62R0203, 1 Cyclotron Road
Berkeley, CA 94720
Phone: (510) 486-6279
E-mail: jbkerr@lbl.gov

[2]Los Alamos National Laboratory (LANL)

[3]3M Fuel Cell Components Program

DOE Manager
HQ: Nancy Garland
Phone: (202) 586-5673
E-mail: Nancy.Garland@ee.doe.gov

Collaborators:
- Adam Weber, Rachel Segalman, John Arnold, Jeff Reimer, Martin Head-Gordon, Robert Kostecki (LBNL)
- James Boncella, Yu Sueng Kim, Jerzy Chlistunoff, Neil Henson, (LANL)
- Radoslav Atanasoski (3M)

Project Start Date: August 31, 2009
Project End Date: August 31, 2013

Fiscal Year (FY) 2011 Objectives

1. Demonstrate that non-platinum group metal (non-PGM) catalysts can be used for oxygen reduction reactions (ORRs) in polymer-coated electrode structures based on polyelectrolyte membranes. (Year 1)

2. Incorporate catalysts into polymer binders of composite electrodes for the construction of membrane electrode assemblies (MEAs) to demonstrate that this is an effective matrix for testing of new catalysts. (Year 2)

3. Demonstrate that the three-dimensional structure of polymer-coated electrocatalyst layers can offset slower kinetics of the catalyst centers when compared with two-dimensional platinum or non-platinum catalysts. (Year 3)

4. Demonstrate that significant stability of the matrix is possible. (Year 3)

5. Demonstrate the design, synthesis and scale up of new catalysts capable of performance that is superior to platinum group metals. (Year 4)

Technical Barriers

This project addresses the following technical barriers from the Fuel Cells section (3.4.4) of the Fuel Cell Technologies Program Multi-Year Research, Development and Demonstration Plan:

(C) Performance – more efficient electrodes
(E) System Thermal and Water Management
(B) Cost
(A) Durability

Technical Targets

- Non-Pt catalyst activity per volume of supported catalyst – 300 A/cm^3
- Cost <$3/kW
- Durability >5,000 hours (>120°C)
- Electrochemical area loss <40%
- Electrochemical support loss <30 mV after 100 hrs @ 1.2 V

FY 2011 Accomplishments

- Completed Objective #1 to demonstrate that non-PGM catalysts can be used for oxygen reduction in polymer-coated electrode structures based on polyelectrolyte membranes.

- Completed Objective #2: Non-PGM catalysts have been incorporated into the polymer binders of composite electrodes used in MEAs and have been shown to support high current densities (up to 0.25 A/cm^2).

- Developed modeling procedures for prediction of MEA performance using non-PGM catalyst layers. The model has been validated by comparison of predicted performance with experiment. The model predicts that Objective #3) will be achieved and this remains to be confirmed experimentally in the coming year.

- Use of redox mediators within the catalyst layers has been shown to be an effective method to reduce the overpotential of the ORR and to increase electron conduction within the catalyst layers.

- Demonstrated methods for mechanistic determination that provides intrinsic catalyst activity. Combination of these methods with molecular modeling and targeted catalyst synthesis has been initiated to provide well defined pathways to lower overpotentials and higher turnover frequencies (TOF).

- Initiated chemical analysis of catalysts using ion trap mass spectroscopy combined with separation methods to assess catalyst degradation pathways and to allow determination of catalyst turnover numbers (TONs).

✧   ✧   ✧   ✧   ✧

Introduction.

Although polymer electrolyte membrane (PEM) fuel cells are relatively efficient energy conversion devices (~50%), there is considerable interest in improving the performance while reducing the cost. An interesting approach is to develop alternative catalysts that are less expensive and also more efficient. Gasteiger and co-workers [1] have provided a very thorough review of the benchmark activities required for Pt, Pt-alloy and non-Pt catalysts for oxygen reduction and which describes in detail different approaches to catalysis of this important reaction. Methods have been reported to prepare non-PGM catalysts that involve a curious procedure whereby a rather complicated molecule such as a metal porphyrin or a complex such as iron phenanthroline is adsorbed on carbon and then heated to over 800°C to form the catalyst [2-5]. In some cases the carbon support is treated with nitrogenous compounds at high temperature followed by addition of metal ions such as Fe or Co. With these non-platinum catalyst structures it is thought that the density of the non-platinum catalytic sites is insufficient to sustain the desired reaction. With the porphyrin catalysts, for example, their poor solubility results in strong adsorption on to the carbon support and insufficient loading of catalyst as well as possible deactivation of the metal center. The pyrolysis process introduces considerable uncertainty as to the actual identity of the catalytic center. Electrode structures are desired which can allow incorporation of catalytic species of known structure into MEAs, which increase the density of the electrocatalysts in the catalyst layer and which allow the homogeneous activity of the catalyst to be retained.

Approach

Homogeneous redox catalysis has been the center of considerable academic attention for several decades and a recent review by Saveant [6] provides an extensive overview of the topic and includes methods of tethering catalysts close to the electrode surface. These methods suggest ways to incorporate into fuel cell MEAs electrocatalysts that mimic very efficient enzyme catalyst centers and may lead to better performance at reduced cost. The principles, advantages and drawbacks behind the approach were explained at greater length in the FY 2010 annual report. The most important advantage of the approach is that the catalyst functions essentially as a homogeneous catalyst that can be thoroughly characterized in solution. This makes design and synthesis of the catalysts more straight forward since they can be studied without resort to surface analysis techniques and to the invocation of surface effects that are poorly understood. Thus, catalysts can be designed from first-principles based on well-known chemistry and physics. The structures of the catalytic centers are understood since the catalysts are synthesized and characterized by classical electrochemical and chemical methods in solution thereby avoiding some of the difficulties that have arisen from surface bound catalysts. The catalysts are then incorporated into polymers for coating on electrode surfaces and again the behavior can be characterized by simple electrochemical methods prior to incorporation of the polymer-bound catalysts into composite electrodes for MEAs. This last step is critical for the project and represents the Go/No-Go decision point that allows the flow of more efficient catalysts into the PEM fuel cell platform for practical use. This report outlines the progress that has been made in the last year towards fabrication of the MEAs and the development of methods and procedures that will lead to better catalysts and improved electrode structures.

Results

Figure 1 illustrates the process of catalyst screening and measurement of kinetic parameters in solution that facilitates some degree of mechanistic determination for the ORR reaction. Figure 1(a) shows the voltammetric response of a representative manganese porphyrin complex (Mn(III) tetramethylpyridylporphine [TMPyP]) which is soluble in aqueous trifluoromethanesulfonic acid solution due to the quaternized pyridinium groups. The Mn(III)/Mn(II) redox couple is shown to be mostly reversible under nitrogen (solid line) but clearly shows two reductive processes which indicates the presence of different species in solution. The relative heights of the reduction peaks vary with sweep rate, addition of chloride ion and also the pH. This behavior contrasts with that shown by the Fe(III)TMPyP complex under the same conditions which shows a simple reversible wave. The dotted line in Figure 1(a) shows the effect of the presence of oxygen in the solution and the increase in the reduction current can be attributed to the catalytic reduction of oxygen by the Mn(II)TMPyP complex. Again there is an anomalous "cross-over" of the current on the anodic sweep which indicates that the reaction is not completely straightforward, probably due to the presence of different catalyst species in solution. Nevertheless from measurements such as these it is possible to estimate the rate constants of the catalytic reactions [6]. Figure 1(b) shows the results of such measurements for several different metal TMPyP complexes plotted against the redox potential of the complex. These rate constants are derived assuming the mechanism shown in Figure 1(c) which assumes an outer-sphere electron transfer between the reduced metal complex and oxygen to form superoxide ion. The dependence on potential shown in Figure 1(b) is consistent with this mechanism but the absolute values of the rate constants are much too high given the potential difference between the catalyst and the superoxide redox potentials. A more likely mechanistic scenario is shown in Figure 1(d) which shows the formation of an intermediate adduct of the complex with oxygen which in this case is shown as a dimer as this is consistent with some of the behavior reported in the literature for these catalysts. It should be noted that the rate of reaction of the catalyst with oxygen is potential dependent and this dependence is actually contrary to what is desirable for a good catalyst.
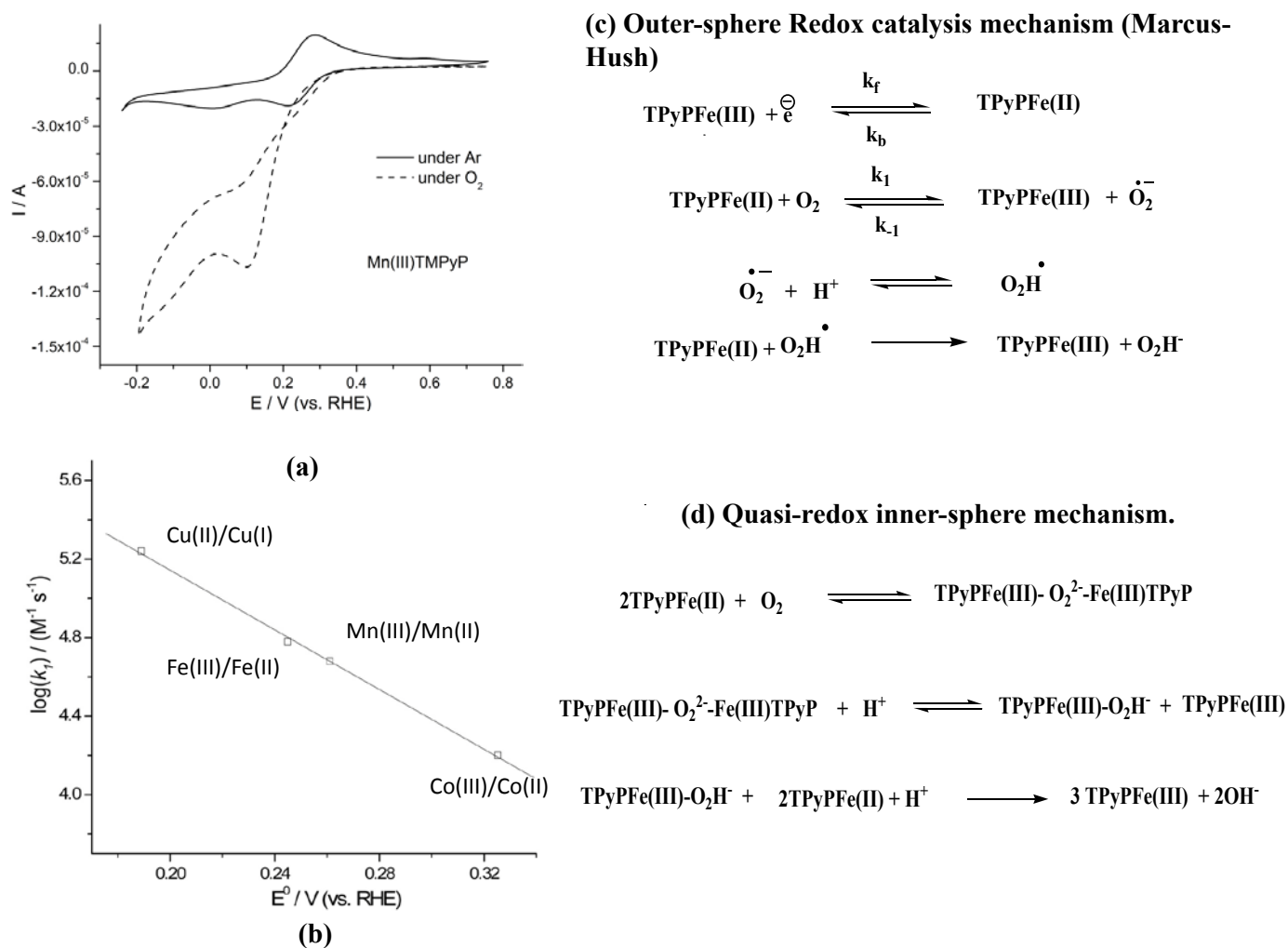
(a)

(b)

(c) Outer-sphere Redox catalysis mechanism (Marcus-Hush)

$$TPyPFe(III) + e^{\ominus} \quad \underset{k_b}{\overset{k_f}{\rightleftharpoons}} \quad TPyPFe(II)$$

$$TPyPFe(II) + O_2 \quad \underset{k_{-1}}{\overset{k_1}{\rightleftharpoons}} \quad TPyPFe(III) + \overset{\bullet}{O_2^-}$$

$$\overset{\bullet}{O_2^-} + H^+ \quad \rightleftharpoons \quad O_2\overset{\bullet}{H}$$

$$TPyPFe(II) + O_2\overset{\bullet}{H} \quad \longrightarrow \quad TPyPFe(III) + O_2H^-$$

(d) Quasi-redox inner-sphere mechanism.

$$2TPyPFe(II) + O_2 \quad \rightleftharpoons \quad TPyPFe(III)\text{-} O_2^{2-}\text{-}Fe(III)TPyP$$

$$TPyPFe(III)\text{-} O_2^{2-}\text{-}Fe(III)TPyP + H^+ \quad \rightleftharpoons \quad TPyPFe(III)\text{-}O_2H^- + TPyPFe(III)$$

$$TPyPFe(III)\text{-}O_2H^- + 2TPyPFe(II) + H^+ \quad \longrightarrow \quad 3\,TPyPFe(III) + 2OH^-$$

FIGURE 1. Electroanalytical screening and characterization of ORR catalysts; (a) voltammetry of Mn(III)TMPyP (0.8mM) in 0.1M HTFSA/water at glassy carbon under argon and in the presence of oxygen, sweep rate 100 mV/s; (b) plot of rate constants for ORR for different metal TMPyP complexes against the redox potential of the catalysts. Kinetic derivation assumes outer-sphere electron transfer mechanism as shown in 1(c); (c) Outer sphere electron transfer mechanism for ORR; (d) postulated quasi-redox inner-sphere mechanism for ORR.

Figure 2(a) shows the voltammetry of the Fe(III)TMPyP catalyst in trifluoromethanesulfonic acid (HTFSA) under argon, in the presence of O_2 and also in the presence of a soluble ferrocene and oxygen. The ferrocene methanol acts as a redox mediator and catalyzes the reduction of oxygen at lower overpotentials. The mechanism whereby this is thought to occur is shown in Figure 2(b). The electron transfer between the ferrocene and the Fe(III)TMPyP catalyst is driven by the rate of the reaction between the reduced catalyst and O_2. The ferrocene also simply acts as an electron mediator to carry the electrons to the catalyst in a polymer layer as is illustrated in Figure 2(c) which schematically shows the FeTMPyP electrostatically bound to Nafion®. Since the catalyst is a 5+ charged cation it is very immobile in the polymer and hence electrons need to be transported to it by some method which the ferrocene fulfills. Figure 2(d) shows how this works in cyclic voltammetry for a Nafion®-coated electrode containing the

FeTMPyP catalyst and the ferrocene methanol which is immersed in HTFSA solution. The freshly cast film (blue line) shows strong catalysis of oxygen reduction at the potential that corresponds to the ferrocene methanol. The film was left immersed in the HTFSA solution for two days and the red line shows the resulting behavior for the ORR. The ORR reaction appears to occur at the potential of the FeTMPyP and other non-catalytic couple appears at more positive potentials. This couple appears to correspond to the ester of the ferrocene alcohol which results from reaction with the Nafion® and yields a shift of the potential in the positive direction consistent with the electron withdrawing nature of the ester. The lack of catalysis by the ferrocene ester is consistent with the mechanism shown in Figure 2(b) as the potential difference between the redox potentials of Fe(III)TMPyP and the ferrocene ester is too large for the rate of the oxygen reaction to overcome. Catalysis over this potential range would be possible if the rate of reaction with
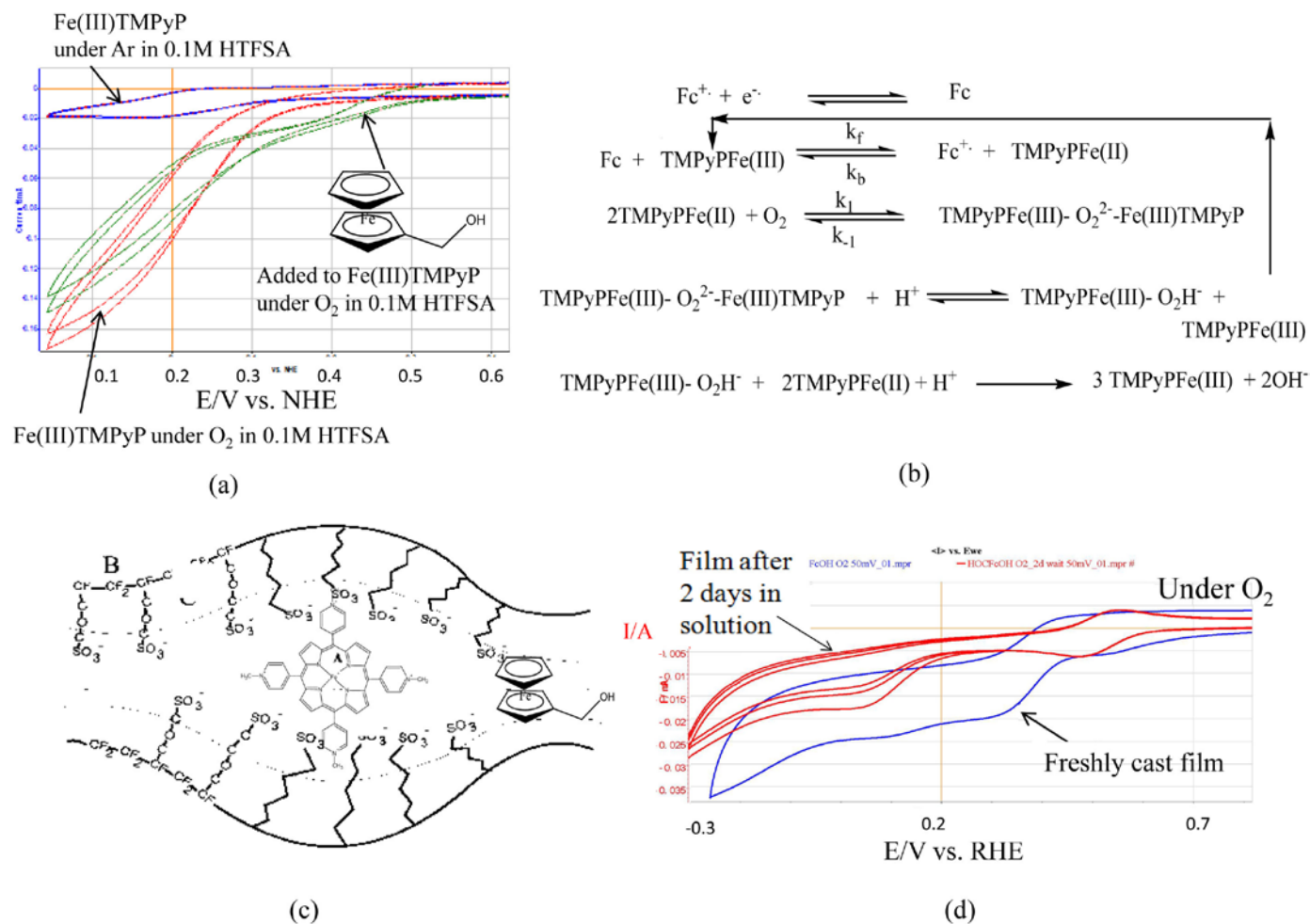
(a)

(b)

(c)

(d)

FIGURE 2. (a) Voltammetry of Fe(III)TMPyP in aqueous 0.1M HTFSA at glassy carbon, sweep rate 50 mV/s showing response under argon, in the presence of oxygen and in the presence of oxygen with added ferrocene methanol; (b) mechanism for ORR with addition of ferrocenemethanol to account for ORR at more positive potentials as shown in Figure 1(a); (c) schematic of Fe(III)TMPyP bound to Nafion® polymer layers which also contain ferrocene methanol as an electron mediator; (d) voltammetric response of freshly cast Nafion® film on a glassy carbon electrode containing Fe(III)TMPyP and ferrocene methanol in aqueous 0.1M HTFSA solution saturated with O_2. Blue curve is freshly cast film, red curve is after two days in 0.1M HTFSA solution.

O_2 was much larger, say two orders of magnitude higher. It is important to note also that both catalyst and mediator appear to remain bound in the polymer layer over an extended period which indicates they do not wash out.

The process of transferring these catalysts into the catalyst layer of an MEA is shown in Figure 3. Figure 3(a) shows the catalyst layer consisting of a number of carbon support particles which are coated with the polymer layer containing the catalyst and mediator. The carbon particles connect electronically to the current collector gas diffusion layer. Figure 3(b) shows the dynamics of the charge and mass transport through the polymer layers that have to be accounted for and Figure 3(c) shows the flow of electrons in simplified form. A number of literature measurements for the transport properties of the electrons, protons, oxygen and water have been have been used to try to predict the behavior of the electrode in an MEA and the results of the

modeling are shown in Figure 3(d) which are compared with experimental results from the polarization curves of MEAs prepared with catalyst layers containing the Fe(III)TMPyP and ferrocene methanol. The model also makes assumptions regarding the overpotential and the catalytic activity of the catalyst. It can be seen that there is surprisingly close agreement for these early results and the model. Figure 3(e) shows the effect of variation of the formulation of the electrode ink where the catalyst concentration is reduced but the mediator concentration remains the same. However, as a result the concentration of proton carriers also decreases. The MEA performance reflects the lower density of the catalysts as well as the increase in resistance due to fewer proton carriers.

Figure 4(a) shows the best MEA performance to date obtained with the Co(III)TMPyP catalyst, ferrocene methanol mediator and different surface area carbons
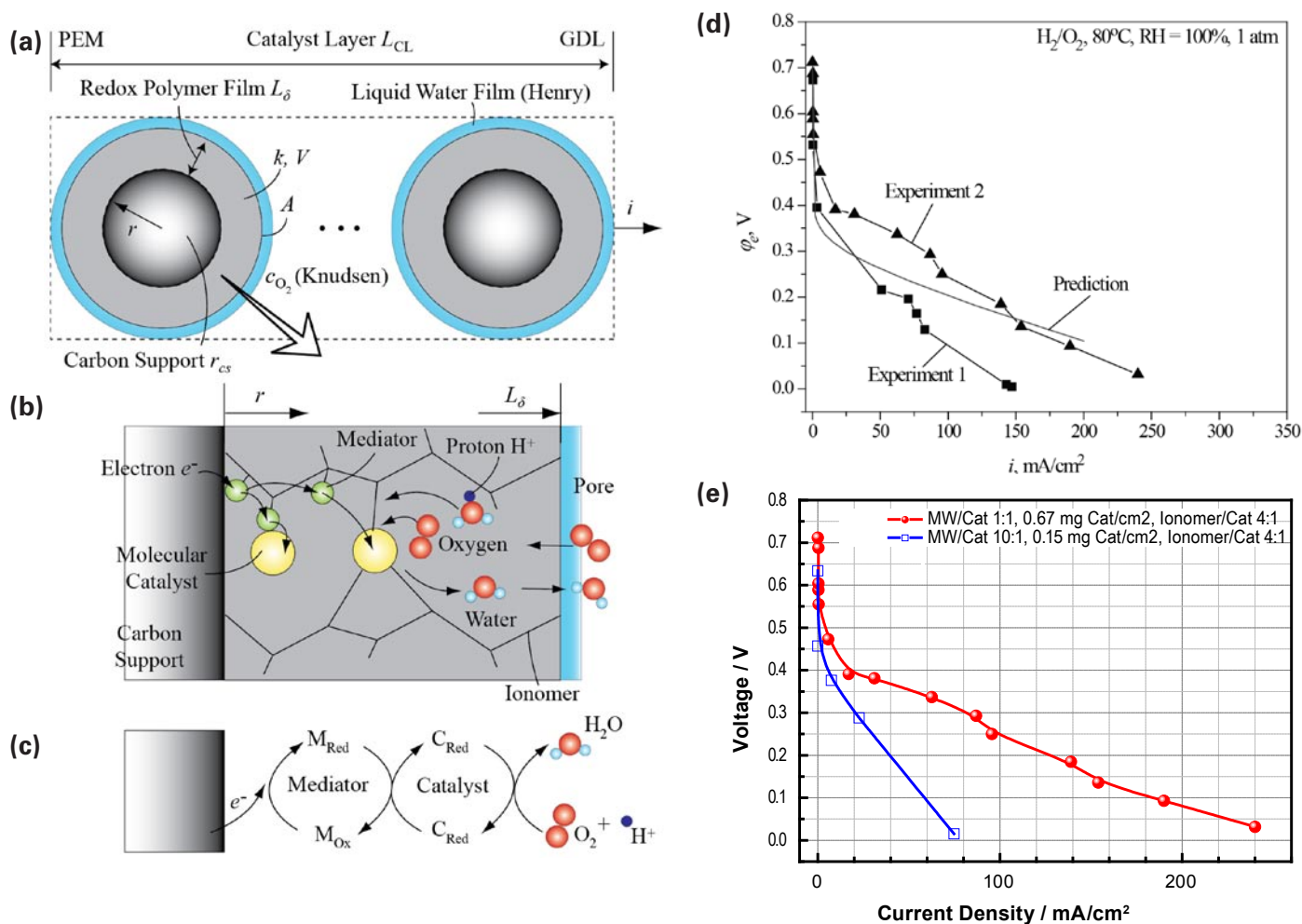
(a) PEM Catalyst Layer L_{CL} GDL

Redox Polymer Film L_δ Liquid Water Film (Henry)

k, V

A

r

c_{O_2} (Knudsen)

i

Carbon Support r_{cs}

(b)

r L_δ

Mediator Proton H$^+$

Electron e^-

Pore

Molecular Catalyst

Oxygen

Carbon Support

Water

Ionomer

(c)

e^-

M_{Red} C_{Red} H$_2$O

Mediator Catalyst

M_{Ox} C_{Red} O$_2$ + H$^+$

(d)

H$_2$/O$_2$, 80°C, RH = 100%, 1 atm

φ_e, V

Experiment 2

Prediction

Experiment 1

i, mA/cm^2

(e)

Voltage / V

MW/Cat 1:1, 0.67 mg Cat/cm2, Ionomer/Cat 4:1
MW/Cat 10:1, 0.15 mg Cat/cm2, Ionomer/Cat 4:1

Current Density / mA/cm^2

FIGURE 3. Model and experimental results of MEA electrodes containing three-dimensional arrays of Fe(III)TMPyP catalysts and ferrocene methanol mediators; (a) schematic of catalyst layer structure; (b) schematic of polymer film structure and dynamics of transport; (c) simplified diagram of electron transport within the catalyst layer; (d) model prediction compared with experimental results for MEA with Fe(III)TMPyP catalyst and ferrocene methanol mediator; (e) MEA results for lower catalyst density, higher mediator density and lower proton carrier density in catalyst layer.

current collectors. Comparison with control experiments with uncatalyzed carbons show an order of magnitude higher current densities and open-circuit voltage values that are 300 mV higher. It is clear that the concept of the polymer-supported homogenous catalyst actually works and the current densities achieved here correspond to TOF numbers of about 10 per second for the catalysts. The actual loading of catalyst sites estimated for these MEAs is about 100 times less than those reported for pyrrolized MEA systems [7]. However, comparison with commercial platinum electrodes (shown in the inset) demonstrates a long way to go, particularly with respect to voltage. Similar current densities as Pt/C TOF values of around 50/s are required or a higher density of catalyst in the catalyst layer. To achieve a lower overpotential and hence higher cell voltage not only are higher rate catalysts required but catalysts with more positive redox potentials are required.

Figure 4(b) illustrates an approach that involves molecular modeling to determine the structural features that control the catalyst redox potential (nature of the metal center, substituents on the ligands) as well as the rate of reaction with the oxygen. Figure 4(b) shows a model of the Fe(II) TMPyP with a fifth ligand (imidazole) bound to the metal and the oxygen occupying the sixth position. Modeling shows some deformation of the ring geometry occurs. It has also been shown that replacement of the quaternary methyls on the pyridines with protons results in slower reaction with O$_2$. These results demonstrate the need for a systematic program of modeling, guided synthesis and electrochemical screening to lead the program towards better catalysts. A more empirical approach is shown in Figure 4(c) which shows the electropolymerization of dipyrromethanes which when combined with cobalt ions gives a polymer catalyst layer with interesting catalytic properties as shown in
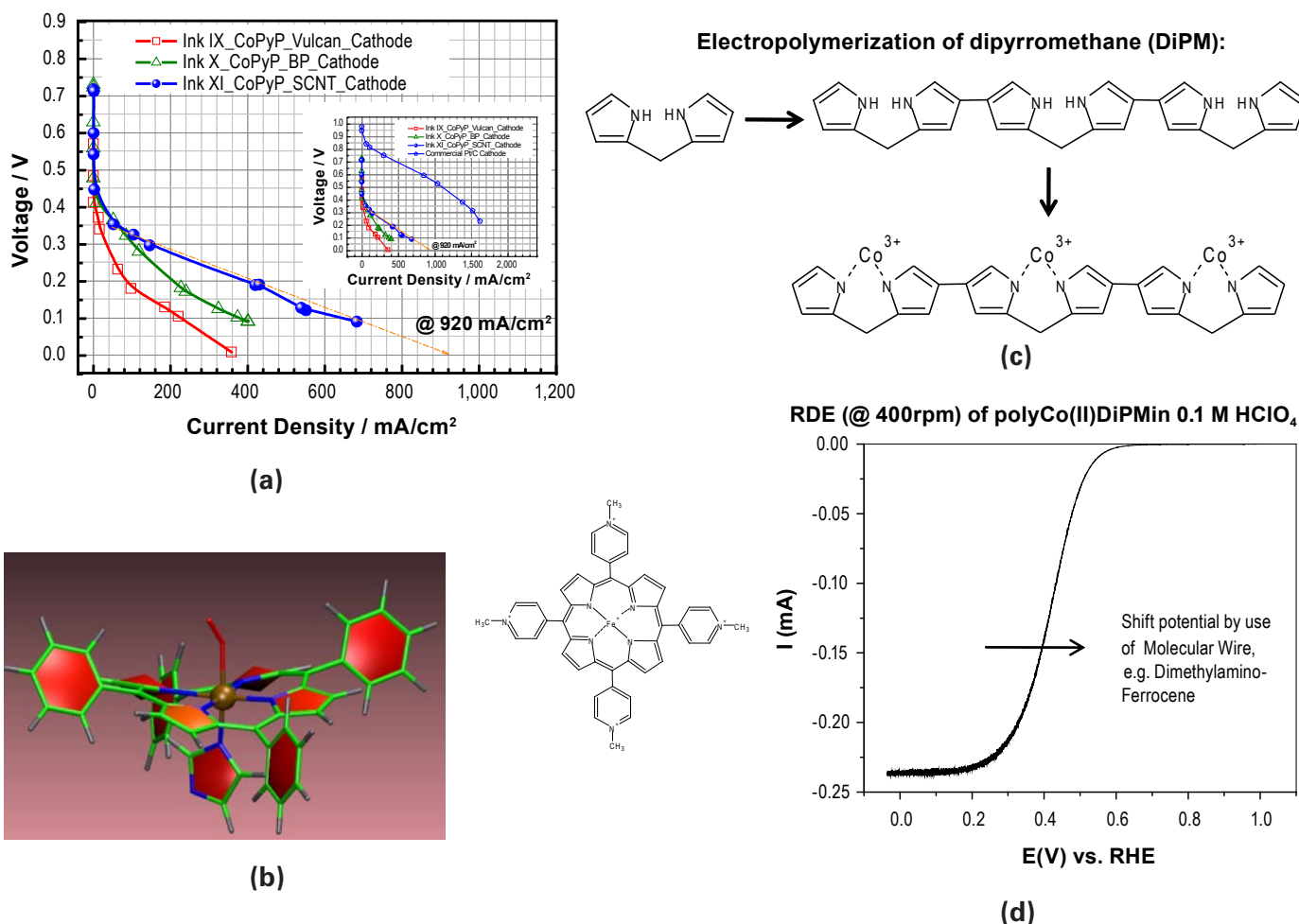
(a)

(b)

Electropolymerization of dipyrromethane (DiPM):

(c)

RDE (@ 400rpm) of polyCo(II)DiPMin 0.1 M HClO$_4$

Shift potential by use of Molecular Wire, e.g. Dimethylamino-Ferrocene

(d)

FIGURE 4. (a) Comparison of MEA results from Figure 3(a) with blank carbon with no added catalyst (control). Inset shows comparison with commercial Pt/C electrode under similar conditions; (b) computational model of FeTMPyP complex with imidazole bound as a fifth ligand and O$_2$ bound to the sixth position; electropolymerization of dipyrromethane and Co^{3+} to form an ORR polymer-catalyst layer; (d) Voltammetric response of catalyst layer formed in 4(c) in the presence of O$_2$.

Figure 4(d). This approach takes advantage of previously successful combination of catalysts with conducting polymers [7]. Combination with redox mediators and proper construction of catalyst layer structures as illustrated in Figure 3 hold the potential to greatly improve the operating potential of the MEA.

Conclusions and Future Directions

Conclusions

- The results from the MEA experiments reported here represent a proof-of-principle of the concept of polymer-supported three-dimensional catalyst arrays for MEA. The correspondence of the modeling with the experimental results indicates that the correct parameters are being considered.

- The correspondence of the MEA results with the electroanalytical results indicates that a practical method catalyst screening exists that is rapid, inexpensive and relevant to MEA operation. Quantitative electroanalytical results are applicable to MEA operation through the electrode modeling.

- Better catalysts can be obtained through fundamental understanding of the factors that influence redox potential and rate of reaction with oxygen. Molecular modeling can address these problems.

Future Directions

- Optimization of MEA fabrication to improve performance.

- Use of electrochemical techniques including impedance to determine rate limiting phenomena in the MEAs and

correlation with electroanalytical measurements made using conventional cell systems.

- Development of a coordinated molecular modeling/ synthesis/electrochemical screening process that will provide understanding of the catalyst structural features that yield better performance.

FY 2011 Publications/Presentations

1. "Molecular-scale, Three-dimensional Non-Platinum Group Metal Electrodes for Catalysis of Fuel Cell Reactions," John Kerr, DOE Fuel Cell Technologies Program Review Meeting, May 10, 2011, Arlington, VA, presentation FC 11.

2. "Development of Low-Temperature Non-Precious Metal Catalysts for Oxygen Reduction." Lior Elbaz and Piotr Zelenay. 219th Electrochemical Society Meeting , Montreal, Quebec, Canada – May 3rd, 2011.

References

1. Gasteiger, H.A., Kocha, S.S., Sompalli, B. & Wagner, F.T. Activity benchmarks and requirements for Pt, Pt-alloy, and non-Pt oxygen reduction catalysts for PEMFCs. *Applied Catalysis B-Environmental* **56**, 9-35 (2005).

2. Gojkovic, S.L., Gupta, S. & Savinell, R.F. Heat-treated iron(III) tetramethoxyphenyl porphyrin supported on high-area carbon as an electrocatalyst for oxygen reduction - I. Characterization of the electrocatalyst. *Journal of the Electrochemical Society* **145**, 3493-3499 (1998).

3. Gojkovic, S.L., Gupta, S. & Savinell, R.F. Heat-treated iron(III) tetramethoxyphenyl porphyrin chloride supported on high-area carbon as an electrocatalyst for oxygen reduction - Part II. Kinetics of oxygen reduction. *Journal of Electroanalytical Chemistry* **462**, 63-72 (1999).

4. Gouerec, P. & Savy, M. Oxygen reduction electrocatalysis: ageing of pyrolyzed cobalt macrocycles dispersed on an active carbon. *Electrochimica Acta* **44**, 2653-2661 (1999).

5. Sun, G.Q., Wang, J.T. & Savinell, R.F. Iron (III) tetramethoxyphenylporphyrin (FeTMPP) as methanol tolerant electrocatalyst for oxygen reduction in direct methanol fuel cells. *J Appl Electrochem* **28**, 1087-1093 (1998).

6. Saveant, J.M. Molecular catalysis of electrochemical reactions. Mechanistic aspects. *Chemical Reviews* **108**, 2348-2378 (2008).

7. Wu, G., More, K.L., Johnston, C.M. & Zelenay, P. High-Performance Electrocatalysts for Oxygen Reduction Derived from Polyaniline, Iron, and Cobalt. *Science* **332**, 443-447, doi:10.1126/science.1200832 (2011).